Quasi-periodic oscillations in the bright Galactic bulge X-ray source GX 340 + 0

van Paradijs, J.; Hasinger, G.; Lewin, W.H.G.; van der Klis, M.; Sztajno, M.; Schulz, N.; Jansen, F.

DOI
10.1093/mnras/231.2.379

Publication date
1988

Published in
Monthly Notices of the Royal Astronomical Society

Mon. Not. R. astr. Soc. (1988) **231**, 379–389

Quasi-periodic oscillations in the bright galactic bulge X-ray source GX 340+0

J. van Paradijs[1], G. Hasinger[2], W. H. G. Lewin[3], M. van der Klis[4], M. Sztajno[2], N. Schulz[2] and F. Jansen[5]

[1]*Astronomical Institute 'Anton Pannekoek', University of Amsterdam, Roetersstraat 15, 1018 WB Amsterdam, The Netherlands*

[2]*Max-Planck-Institut für Extraterrestrische Physik, 8046 Garching bei München, Federal Republic of Germany*

[3]*Center for Space Research and Department of Physics, Massachusetts Institute of Technology 37-627, Cambridge, MA 02139, USA*

[4]*Exosat Observatory, Space Science Department of ESA, ESTEC, Postbus 299, 2200 AG Noordwijk, The Netherlands*

[5]*SRON Space Research Laboratory, Huygens Laboratory, Niels Bohrweg 2, 2300 RA Leiden, The Netherlands*

Accepted 1987 September 18. Received 1987 September 2; in original form 1987 July 12

Summary. GX 340+0 was observed with *EXOSAT* for 13 hr in 1985 and for 12 hr in 1986. During the 1985 observations the spectral state (in the spectral hardness–intensity diagram) varied between the horizontal branch and the upper end of the normal branch; no QPO were observed (however, the time resolution was only 31 ms). During the 1986 observations (the time resolution was 1 ms) the spectral state corresponded to the normal branch and 5.6 Hz QPO were observed (the equivalent sinusoidal rms variation was about 1.8 per cent), but only when the spectral hardness was within a certain range which covered approximately the middle one-third of the normal branch. Very low frequency noise (VLFN) below 0.1 Hz was observed during both observations in all spectral states. The VLFN in the power density spectra could be well fitted by a power law (the slopes were different for the two observations). Red noise (above 0.5 Hz) was exclusively observed during the 1985 observations; its strength increased from $\lesssim$1.5 to 3 per cent as the spectral state changed from the normal to the horizontal branch. This behaviour is similar to that in Cyg X-2 and GX 5−1 which also show approximately 5–6 Hz QPO in the normal branch, red noise above 0.5 Hz (with associated high-frequency 20–50 Hz intensity-dependent QPO) in the horizontal branch, and VLFN in both branches. It thus appears that GX 340+0 is similar in

its QPO behaviour to Cyg X-2 and GX 5−1 (possibly also to GX 17+2), and we suspect that high-frequency QPO was present during our 1985 observations when the source was in the horizontal branch, but that our time resolution of 31 ms was insufficient to detect it. Future observations will show whether high-frequency QPO is present during the horizontal branch state as we suspect.

1 Introduction

GX 340+0 belongs to the class of the bright galactic bulge X-ray sources. Its (2–11 keV) X-ray flux varies irregularly in the range between about 4×10^{-9} and about 1.5×10^{-8} erg cm^{-2} s^{-1} (Forman *et al.* 1978; Markert *et al.* 1979; Warwick *et al.* 1981; Wood *et al.* 1984). There was no evidence for periodicity in the frequency range from 0.2 to 100 Hz (upper limits were 10 per cent; Rappaport *et al.* 1971). The orbital period of the system is unknown.

GX 340+0 has a rather soft X-ray spectrum, characteristic of galactic bulge X-ray sources. Margon *et al.* (1971) found that its spectrum, observed during a rocket flight, could be fitted with a blackbody spectrum, with a blackbody radius of about 8 km (at an assumed distance of 4 kpc). In subsequent studies, based on data with better spectral resolution, acceptable fits to a thermal bremsstrahlung spectrum have been reported with kT values of about 5 keV (Jones 1977; Parsignault & Grindlay 1978; Ercan & Cruise 1984). There is also some evidence for Fe-line emission at 6.7 keV (Parsignault & Grindlay 1978; Ercan & Cruise 1984). The X-ray spectrum shows a low-energy cut-off near 2.5–3.0 keV, corresponding to an equivalent hydrogen column density of about 10^{23} cm^{-2} (Ercan & Cruise 1984; Hertz & Grindlay 1984). A positive correlation between the X-ray intensity of GX 340+0 and the hardness of its X-ray spectrum was reported by Ponman (1982).

No optical counterpart has been found to date; this is probably due to the large interstellar extinction ($A_V \gtrsim 10$ mag) inferred from the low-energy cut-off in the X-ray spectrum (Gorenstein 1975; Ryter, Cesarsky & Audouze 1975). Radio emission has not been detected from GX 340+0 [at 6 cm a 3-sigma upper limit of 0.53 mJy was reported by Grindlay & Seaquist (1986)].

Quasi-periodic oscillations (QPO) with frequencies in the range from about 1 Hz to about 100 Hz, often accompanied by red noise (in the range $\lesssim 10$ Hz), have been detected in the X-ray flux of most of the bright galactic bulge X-ray sources (van der Klis *et al.* 1985; for recent reviews see van der Klis 1987; Lewin & van Paradijs 1986; Stella 1986; Hasinger 1987a, b; Lewin 1987a, b).

We have detected QPO in the X-ray flux of GX 340+0 (some preliminary results were earlier reported in an *IAU Circular* by van Paradijs *et al.* 1987). In this paper we give a detailed description of the QPO, and the associated red noise,* and their relation to the spectral state of the source. The observations are described in Section 2. In Sections 3 and 4 we present the results of the analysis of GX 340+0. The results are discussed in Section 5; Section 6 summarizes our conclusions.

2 Observations

We observed GX 340+0 continuously with *EXOSAT* for approximately 12 hr from 1986 April 6, 20:04 UT to April 7, 08:20 UT. In this paper we discuss data taken with the full array (seven detectors, effective area about 1400 cm^2) of the medium energy (ME) argon detector (Turner, Smith & Zimmermann 1981). The ME data were recorded continuously with a time resolution of

*We use the term red noise to indicate broadband power which increases toward lower frequencies (not necessarily as a $1/f$ power law). In the discussion section we distinguish between low-frequency noise (LFN) and very low frequency noise (VLFN), which have quite different properties (van der Klis *et al.* 1987a; Hasinger 1987b).

about 1 ms (1/1024 s), in the energy range between 1 and 16 keV. Detailed spectral information is available from the ME data (64 energy channels) taken with a time resolution of 0.625 s.

In addition, we analysed approximately 13 hr of archival *EXOSAT* data, taken between 1985 March 29, 16:35 UT, and March 30, 05:28 UT. During these observations one half of the ME array (four detectors) was always pointed at the source, with the other half offset by approximately two degrees to monitor the background. The two array halves were interchanged ('array swaps') three times during the observations. Data were also recorded continuously in one energy channel (1–16 keV) with a time resolution of 31.25 ms. During these observations spectral information was provided by the ME data in 32 energy channels with a time resolution of 10 s.

3 Spectral analysis

The X-ray light curves (ME counting rate in the 2–15 keV energy interval), as obtained in 1985 and 1986, are shown in Fig. 1 (the background is subtracted, and dead-time corrections have been made). During these observations the counting rate (normalized to the full array of eight detectors) varied between approximately 1400 and 1550 ct s^{-1}, and between approximately 1000 and 1450 ct s^{-1}, respectively. The background for the low time resolution data in the energy interval (1–15 keV) where most of the source signal is contained was about 50 ct s^{-1} for the full array. This was estimated from the counting rates as observed in the array half offset from the source (1985 data), and during slews of the satellite between source pointings (1986 data). For the high time resolution data the background counting rates were about 80 ct s^{-1} (1986 data) and about 600 ct s^{-1} (1985 data; these include the background counts from the xenon detectors).

In Fig. 2 we show the relation between the hardness of the X-ray spectrum (measured by a 'hardness ratio', equal to the ratio of background- and dead-time-corrected counting rates in the

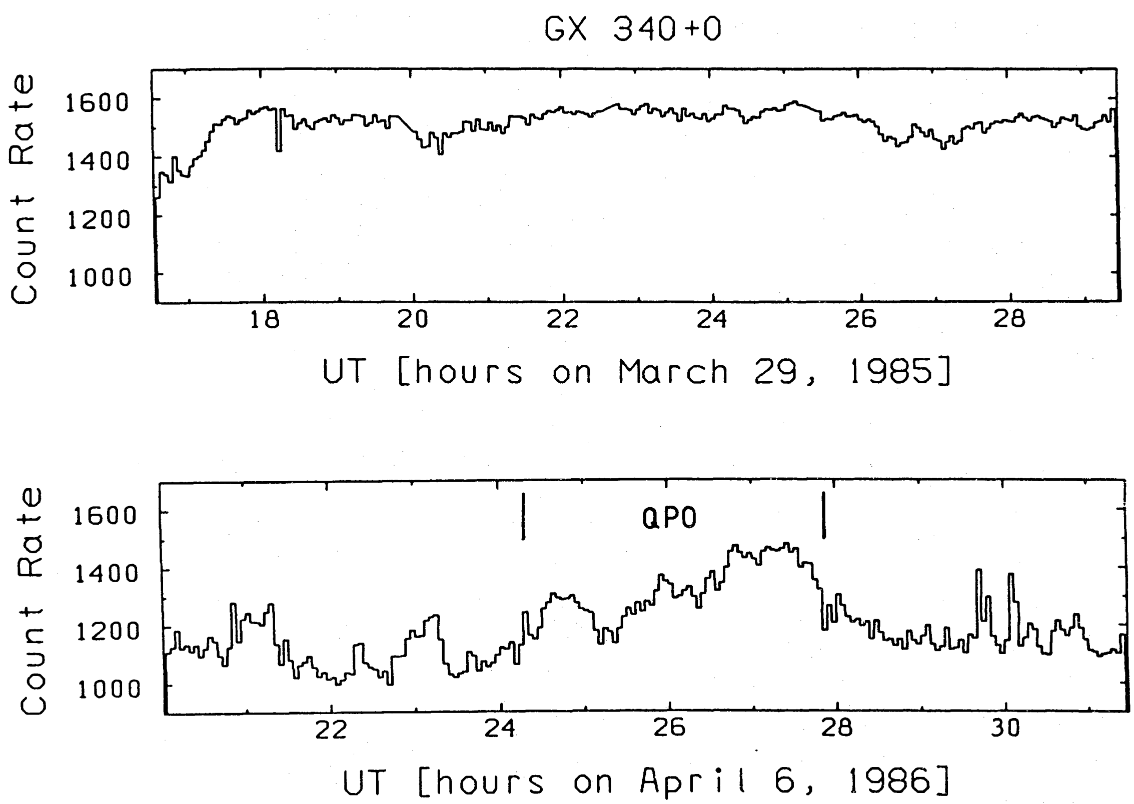

Figure 1. Light curves (ct s^{-1}, 2–15 keV) for the March 1985 and April 1986 observations.

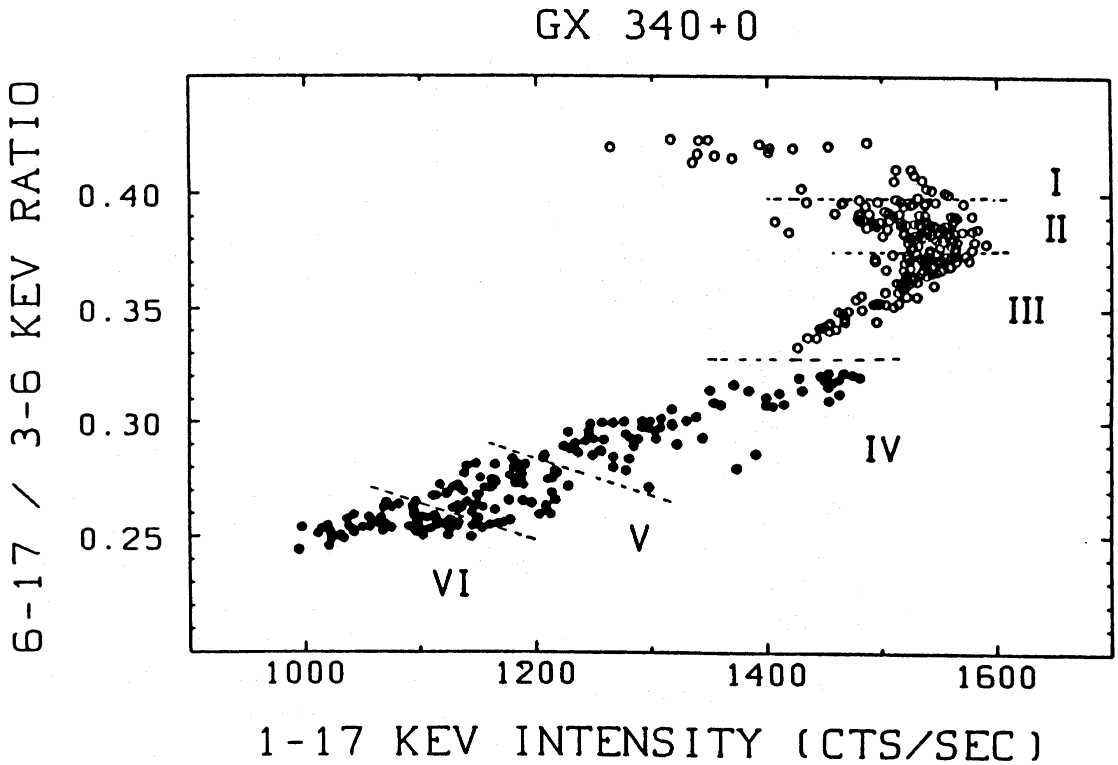

Figure 2. Spectral hardness–intensity diagram. The filled circles represent the 1986 data, the open circles the 1985 data. The data were divided in six sets (see text), they are indicated with roman numerals in this figure.

energy ranges 6–17 and 3–6 keV) and the 1–17 keV counting rate. During the 1986 observations (solid circles in Fig. 2) the hardness ratio was positively correlated with the X-ray intensity (the source was on the so-called 'normal branch'; see, for example, Shibazaki & Mitsuda 1984; van der Klis *et al.* 1987a; Hasinger 1987a). During the 1985 observations (open circles) the spectral state of the source corresponded to the upper part of the normal branch, and the turnover to the 'horizontal branch' (on which the X-ray spectrum is relatively hard, and does not change much with the source intensity). The two branches in the hardness–intensity diagram are smoothly connected at an 'apex' in the upper right-hand corner of the diagram.

We have made a spectral analysis of six data sets, indicated by Roman numerals I–VI (see Fig. 2; QPO is detected only in data set IV, see next section). After correcting for instrumental dead-time, and subtracting the background, we fitted the ME data (64 channels) with a three-component spectral model (which also includes interstellar absorption), consisting of a blackbody, a thermal bremsstrahlung spectrum, and an Fe-emission line at 6.7 keV, with a fixed full width at half maximum of 0.5 keV.

The results of the spectral fits are listed in Table 1 (the quoted errors are one-sigma, and take the correlations between the parameters into account). From this table it appears that along the track in the hardness–intensity diagram (see Fig. 2) the largest change occurs in the temperature of the thermal bremsstrahlung component (between about 5 keV at the lower-left part of the normal branch, to about 10 keV on the horizontal branch). The blackbody temperature changes only by about 10 per cent. The fractions of the blackbody component to the total flux (2–15 keV) were 0.26 ± 0.06 on the horizontal branch (data set I in Fig. 2) and 0.33 ± 0.08 in the lower part of the normal branch (data sets V and VI of Fig. 2). The difference is not significant. The average (over all six sections) iron line intensity was 2.5 ± 0.6 photons $cm^{-2} s^{-1}$, corresponding to an equivalent width of about 50 eV.

The equivalent hydrogen column density is comparable in the two observations. Its average value, $N_H = 4.8 \pm 0.3 \times 10^{22}$ cm^{-2}, is consistent with values previously reported (Ercan & Cruise 1984; Hertz & Grindlay 1984).

For the observed spectral shapes 1 ct s^{-1} in the ME detector corresponds to a 2–11 keV X-ray flux of approximately 6.9×10^{-12} and 8.8×10^{-12} erg cm^{-2} s^{-1} for the 1985 and 1986 data, respectively. Thus, the X-ray flux varied between about 0.9×10^{-8} and 1.3×10^{-8} erg cm^{-2} s^{-1} (2–11 keV), which is within the range previously observed.

4 Timing analysis

We have estimated the power spectra of the intensity variations by calculating the Fourier amplitudes via a Fast Fourier Transform algorithm. The power spectra were normalized following Leahy *et al.* (1983), i.e. the power density in Poissonian noise is expected to be equal to 2.0. Detector dead-time effects will cause the distribution to deviate slightly from a purely Poissonian distribution, and the power to be slightly lower; these effects are taken into account (see below).

To look for the possible presence of high-frequency coherent pulsations, power spectra were calculated for the 1986 data for individual data blocks containing 2^{15} samples of 0.98 ms. There is no evidence for coherent pulsations in the average power spectra, with 99 per cent confidence level upper limits to the rms variation of 0.5–0.7 per cent in the range between 0.03 and 500 Hz. These limits do not take into account the possible Doppler smearing due to orbital motion. For an orbital period of ~10 days (e.g. Cyg X-2) this effect can be neglected, while for an orbital period of 11 min (e.g. 4U 1820−30) the upper limits have to be increased by roughly a factor of 5 at the highest frequencies.

From an inspection of a colour-coded display of power spectra versus time (see van der Klis *et al.* 1985), we obtained clear evidence for the presence of QPO during an approximately 3.5 hr period during the 1986 observations, when the X-ray intensity was relatively high. The QPO became detectable when the source intensity (1–17 keV) increased above about 1250 ct s^{-1}, and became undetectable when it decreased below this value about 3.5 hr later (see Fig. 1). This was confirmed by making a display of the power spectra in which they are ordered according to X-ray intensity. From this it was clear that QPO were only detected when the source intensity was between about 1250 and about 1450 ct s^{-1}. Independent of the presence or absence of QPO, there is clear evidence for red noise (below about 0.1 Hz) throughout the 1985 and the 1986 observations.

To study the broadband characteristics of the power spectra (i.e. the QPO, and the red-noise properties) power spectra were calculated for individual 256 and 8 s data blocks, for the 1985 and 1986 data, with time resolutions of 31.25 and 0.98 ms (8192 samples), respectively. These power spectra were averaged over six data sets (see Fig. 2, and below), and rebinned into logarithmically equidistant frequency bins. In order to extend the frequency range to very low frequencies, we repeated the same procedure by rebinning the 1985 data by a factor of 4 (1024 s data blocks, and 125 ms time resolution; the lowest frequency was 10^{-3} Hz), and the 1986 data by factors of 64 and 128 (the lowest frequencies were 2×10^{-3}, and 4×10^{-3} Hz).

We analysed the average power spectra for the six sets of data (indicated by I–VI in Fig. 2), which were also used in the spectral analysis (see Section 3). The total number of data blocks in sets I–III, and sets IV–VI, are 14, 80 and 67 (of 256 s each), and 1911, 1480 and 1674 (of 8 s each), respectively. These power spectra cover the frequency ranges 4×10^{-3} to 16 Hz, and 4×10^{-3} to 512 Hz, for the 1985 and the 1986 data, respectively. The errors in the averaged power density spectra were determined from the distributions (for each individual frequency bin separately) of the power density estimates in the individual power spectra.

In order to describe the power spectra quantitatively we have made least-squares fits to average

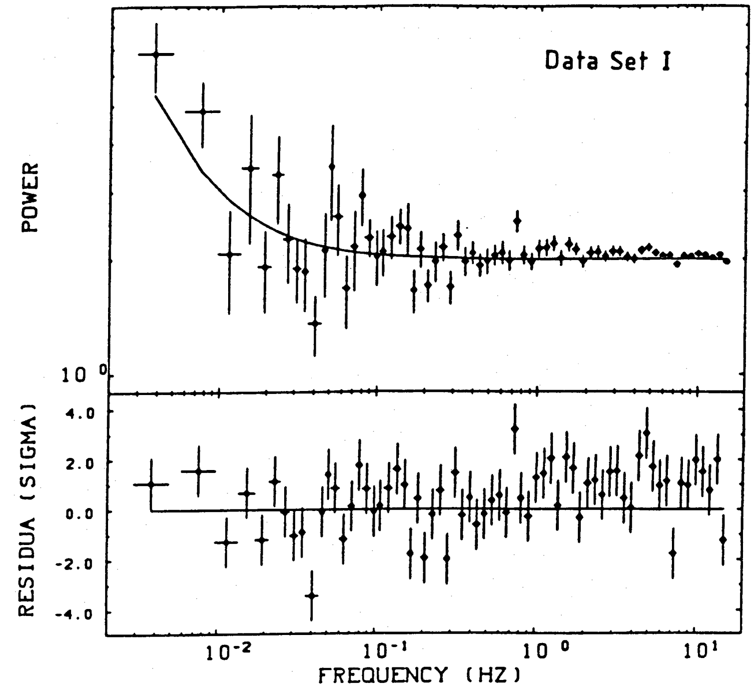

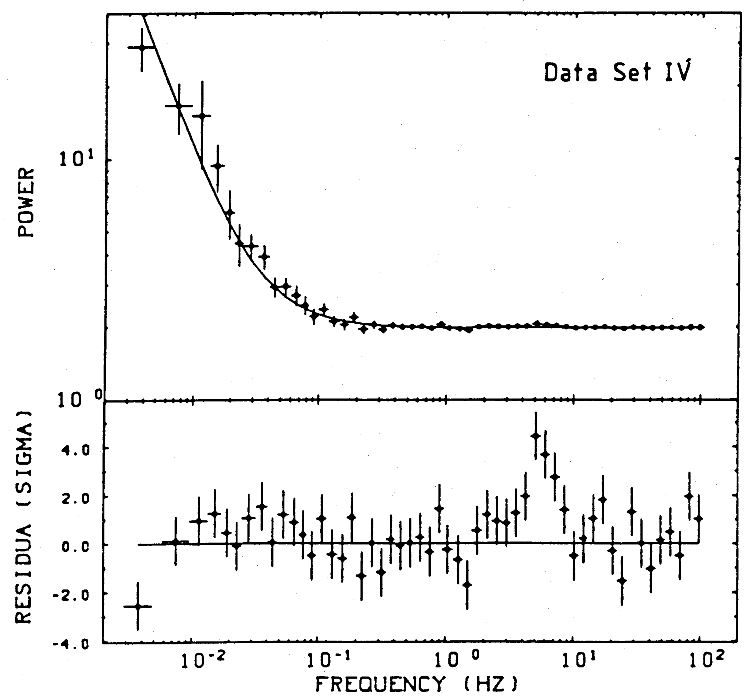

Figure 3. Power-density spectra, for data from set I (upper panel) when the source was on the horizontal branch, and set IV (lower panel) when the source was on the normal branch and 5.6-Hz QPO was observed (see Fig. 2). The solid lines indicate the fits (see text). The difference between the data and the fits are shown at the bottom of each panel in terms of the number of standard deviations. The excess red noise above 0.5 Hz can be seen in the upper panel. The 5.6-Hz QPO can be seen in the bottom part of the lower panel.

power spectra, using a fitting function in which the QPO is described by a Lorentzian profile (with centroid frequency $F_{(QPO)}$, and full width at half maximum W), the red noise by a power law with exponent Γ. The noise level was fixed to a value which varied between 1.994 and 1.997, depending on dead-time (see Tennant 1987).

Table 1. Spectral and timing results for GX 340+0.

Set	Time	N_H	F_{bb}	kT_{bb}	F_{th}	kT_{th}	F_{bb}/F_{tot}	A^a_{VLFN}	A^b_{LFN}	A^c_{QPO}	A^d_{QPO}
	[s]	[$10^{21}cm^{-2}$]	(e)	[keV]	(e)	[keV]	(f)	[%]^g	[%]^g	[%]^g	[%]^g
I	3584	50.9 ± 2.7	2.0 ± 0.4	1.31 ± 0.04	5.8 ± 1.1	10.3 ± 1.7	0.26 ± 0.06	0.86 ± 0.15	3.2 ± 0.3	$< 2.5^h$	–
II	20480	51.2 ± 2.4	2.3 ± 0.4	1.34 ± 0.03	5.5 ± 0.8	8.5 ± 1.0	0.30 ± 0.05	0.66 ± 0.07	2.0 ± 0.2	$< 1.5^h$	–
III	17152	51.5 ± 2.6	2.3 ± 0.4	1.29 ± 0.03	5.3 ± 1.0	7.9 ± 0.9	0.31 ± 0.06	0.68 ± 0.07	1.6 ± 0.3	$< 1.8^h$	–
IV	15288	46.6 ± 2.8	1.8 ± 0.4	1.20 ± 0.04	4.1 ± 0.7	5.6 ± 0.6	0.31 ± 0.07	1.18 ± 0.05	$< 1.3^h$	1.77 ± 0.18	$< 1.4^h$
V	11840	45.6 ± 1.8	1.7 ± 0.4	1.14 ± 0.04	3.3 ± 0.7	5.0 ± 0.5	0.34 ± 0.07	1.67 ± 0.06	$< 1.3^h$	$< 1.0^h$	$< 2.2^h$
VI	13392	45.3 ± 3.1	1.5 ± 0.4	1.11 ± 0.03	3.0 ± 0.7	4.7 ± 0.5	0.33 ± 0.08	1.49 ± 0.10	1.6 ± 0.2	$< 1.3^h$	$< 1.5^h$

(*a*) $4 \cdot 10^{-3} - 0.1$ *Hz*
(*b*) $0.5 - 10$ *Hz*
(*c*) QPO peak at 5.6 Hz with width 2.7 Hz
(*d*) QPO peak at 40 Hz with width 12 Hz
(*e*) keV/cm^2s ($2 - 15$ keV); $1keV = 1.6 \cdot 10^{-9}erg$
(*f*) $2 - 15keV$
(*g*) equivalent sinusoidal rms. variation
(*h*) 2 σ upper limits

Fits to two of these power spectra (sets I and IV) are shown in Fig. 3. QPO were seen only in data set IV (the change in chi-squared when the Lorentzian is added is 36.9 for 49 degrees of freedom). The best-fit values for the parameters of the QPO are $F_{(QPO)} = 5.6 \pm 0.3$ Hz, and $W = 2.7 \pm 0.9$ Hz. The power in the QPO (above the red-noise and the white-noise level) corresponds to an equivalent sinusoidal rms variation of 1.8 ± 0.2 per cent; these are one-sigma single-parameter errors, which take into account the correlation between the parameters. The QPO parameters are very insensitive to the red-noise parameters.

Two-sigma upper limits, p_0 (in per cent) to the equivalent sinusoidal rms variations for QPO in data sets I–III, and V–VI (with the same centroid frequency and FWHM as those detected in data set IV) are given in Table 1. For a different centroid frequency of F(Hz), and a different width (FWHM) of W(Hz), the upper limit, p(per cent), is approximately given by

$$p = p_0 (W/2.7)^{1/2} (F/5.6)^{-1/4}.$$

In addition, Table 1 contains the two-sigma upper limits to the rms variation of QPO with $F = 40$ Hz, and $W = 12$ Hz (as observed in GX 5−1 and Cyg X-2 during the horizontal-branch spectral state; see van der Klis *et al.* 1985; Hasinger *et al.* 1986).

Red noise is clearly visible below 0.1 Hz; it could be well fitted by a power law, $P(F) \propto F^{-\Gamma}$. The value of Γ was determined from the overall average power spectra of the 1985 and 1986 observations independently; these power spectra cover the frequency range 10^{-3} to 16 Hz, and 2×10^{-3} to 512 Hz, respectively. The best-fit values of Γ are 1.23 ± 0.11 (1985 data), and 1.58 ± 0.04 (1986 data). Fitting the above power law to the individual data sets (I–VI) does not yield meaningful results because in the reduced frequency interval the power-law slope is poorly defined. In determining the rms variation of the red noise for data sets I–VI, we integrated the excess power (above the white-noise level) in the frequency range 4×10^{-3} to 10^{-1} Hz (we estimate that the contribution of the 0.5–10 Hz excess power, discussed below, is less than 10 per cent). The resulting values of the rms variation of the power-law red noise (in the frequency range 10^{-3} to 10^2 Hz) are listed in Table 1. It appears that the rms intensity variation in the power-law red-noise component was somewhat smaller during the 1985 observation ($\lesssim 1$ per cent) than during the 1986 observations (1–1.7 per cent).

The 1986 data allow a study of the photon energy dependence of the red-noise component. We

Table 2. Energy dependence of VLFN (combined data sets IV–VI).

Energy band (keV)	Γ_{VLFN}*	A_{VLFN} (per cent)†
1–17	1.55±0.04	2.75±0.07
1–3	1.64±0.09	2.06±0.15
3–6	1.56±0.05	2.91±0.08
6–17	1.51±0.05	3.67±0.11

*Power-law index (see text).
†Equivalent sinusoidal rms variation (10^{-3}–100 Hz).

have made separate power spectra, using the energy-resolved 0.63-s time resolution data, for the photon energy intervals 1–3, 3–6 and 6–10 keV, respectively. We fitted a power law to the red noise without any restriction on the level of the white noise. We found (see Table 2) that the rms intensity variation in the red noise increased by a factor of about 2 towards high energies. The exponent Γ of the power law does not show a significant dependence on photon energy.

The power spectra for some of the six data sets show broadband power at frequencies roughly between 0.5 and 10 Hz, in excess of the white-noise level. The contribution of the above power law is negligible in this frequency range. The signal is insufficient to perform model least-squares fits; we therefore determined the excess power in the frequency range 0.5–10 Hz by integrating the power density (after subtracting the white-noise level and the QPO, if present). The results (see Table 1) show that the rms variation in the range 0.5–10 Hz decreases systematically from about 3 to $\lesssim$1.5 per cent, when going from the horizontal branch to the normal branch in the hardness–intensity diagram.

5 Discussion

During the time intervals covered by the observations reported here, GX 340+0 showed a bimodal spectral behaviour, which has previously been observed for other low-mass X-ray binaries (see e.g. Branduardi *et al.* 1980; Shibazaki & Mitsuda 1984; Hasinger 1987a; van der Klis *et al.* 1987a; Lewin *et al.* 1987a; Penninx *et al.* 1987). During about two-thirds of the time the source was on the normal branch, during about 10 per cent of the time on the horizontal branch, and the remaining time was spent in the transition region ('apex') between these two branches (Fig. 2). The ratio of the 1–17 keV intensity (in ct s^{-1}) at apex to that at the left end of the horizontal branch is approximately 1.2. In comparison with Cyg X-2 and GX 5−1, for which these ratios range between 1.65 and 1.8 (Hasinger 1987a; van der Klis *et al.* 1987a) it seems possible (but this is uncertain, as the origin of the branches is unknown) that GX 340+0 covered only the high intensity part of the horizontal branch.

The QPO behaviour in several low-mass X-ray binaries is bimodal, e.g. GX 5−1 (van der Klis *et al.* 1987a), Sco X-1 (Priedhorsky *et al.* 1986; van der Klis *et al.* 1987b), Cyg X-2 (Hasinger 1987a; Hasinger *et al.* 1987, in preparation), and GX 17+2 (Stella, Parmar & White 1987) and is correlated with their bimodal spectral behaviour.

In GX 5−1 and Cyg X-2, intensity-dependent high-frequency (20–50 Hz) QPO accompanied by 'low-frequency-noise' (LFN) extending to frequencies about as high as the QPO frequency, is observed during the horizontal-branch spectral state. During the normal-branch spectral state, the QPO frequency is much lower (typically 5–10 Hz) in these two sources, and the LFN above about 0.5 Hz is not observed (Norris & Wood 1987; Hasinger *et al.* 1987, in preparation; van der

Klis *et al.* 1987a; Tanaka, private communication). These 'normal branch' QPO have also been observed in GX 349+2 (Lewin *et al.* 1985, 1987b; Cooke, Stella & Ponman 1985), and in GX 3+1 (Lewin *et al.* 1987a).

Bimodal QPO behaviour has also been observed in Sco X-1 (Priedhorsky *et al.* 1986), and in GX 17+2 (Stella *et al.* 1987), but the QPO characteristics do not appear to fit the (Cyg X-2/GX 5−1) normal- and horizontal-branch behaviour. There is, however, recent evidence that the bimodal behaviour in Sco X-1 and GX 17+2 do fit the Cyg X-2/GX 5−1 scheme; the 6-Hz QPO in Sco X-1, and the 7-Hz QPO in GX 17+2 would then be associated with the normal branch (*cf.* Hasinger 1987b).

A steep 'very low frequency noise' (VLFN) component is observed in the power spectrum of several sources, which is particularly prominent below ~0.1 Hz, and does not appear to be correlated with the presence of QPO. The frequency dependence of this VLFN can often be described by a power law with a slope in the range 1.2–1.7 (see the above references to individual sources, and Makishima 1986). The equivalent sinusoidal rms variation of the VLFN, which is typically 1.5–3 per cent (for the 1–10 keV energy range) increases substantially more slowly with photon energy than that of the QPO-related, and higher frequency, red noise (see e.g. van der Klis 1987; Hasinger *et al.* 1987, in preparation).

QPO were only observed when GX 340+0 was near the central part of the normal branch (data set IV, see Fig. 2). The centroid frequency and FWHM of the QPO peak in the power spectrum were 5.6±0.3 Hz, and 2.7±0.9 Hz, respectively. The equivalent sinusoidal rms modulation in these QPOs was 1.8±0.2 per cent. In the other data sets no QPO were detected, with upper limits to their rms variation between typically about 1 and 2.5 per cent. When the source was in the horizontal branch the time resolution of the data was not sufficient to detect QPO in the 20–50 Hz range, in which the horizontal-branch QPO of GX 5−1 and Cyg X-2 were detected.

The 5.6 Hz QPO detected in GX 340+0 are similar to the 'normal-branch' QPO, with frequencies in the range between about 5 and 10 Hz, which have been observed during the normal-branch spectral state in many other QPO sources (see above).

During both GX 340+0 observations, the power spectrum showed red noise below about 0.1 Hz, which could be well fitted by a power law. The exponent of this power law, and the rms variation of the red noise are similar to the corresponding values observed for the very low frequency noise (VLFN) component in the power spectra of several other QPO sources (see above). The strength of this noise component, which does not show a strong dependence on the spectral state of the source, nor on the presence or absence of QPO, increases with photon energy by a factor of about 2 over the range of about 2–10 keV. Thus, the noise component that we observed in GX 340+0 (and which was always present) can very plausibly be identified with the above VLFN component.

When GX 340+0 makes a transition from the normal branch to the horizontal branch, excess power appears in the power spectrum at frequencies above about 0.5 Hz, which increases in strength when the source moves toward the horizontal branch. Our data do not allow us to measure the exact shape nor the energy dependence of the 0.5–10 Hz excess power.

The high-frequency (20–50 Hz) QPO observed in GX 5−1 and Cyg X-2 during the horizontal-branch state is correlated with a characteristically shaped LFN component which extends to much higher frequencies than the above VLFN. This LFN component, whose strength strongly increases with photon energy, is not observed when these sources are in the normal-branch state (van der Klis *et al.* 1987a; Hasinger 1987b). Thus, the appearance of excess power in the 0.5–10 Hz range, when GX 340+0 moved on to the horizontal branch, suggests that high-frequency QPO was present, but was unobservable because of the time resolution of 31 ms during the 1985 observations. Future observations will be able to confirm our expectation that high-frequency QPO is present when GX 340+0 is in the horizontal-branch state.

6 Conclusions

During the 1985 *EXOSAT* observations of GX 340+0 the spectral state (in the spectral hardness–intensity diagram) varied between the horizontal branch and the upper end of the normal branch; no QPO were observed (however, the time resolution of the 1985 data was only 31 ms). During the 1986 observations the spectral state varied along the normal branch and 5.6-Hz QPO were observed (rms variation about 1.8 per cent), but only when the spectral hardness was within a certain range which covered approximately the middle one-third of the normal branch. VLFN below 0.1 Hz was observed during both observations in all spectral states. The VLFN could be well fitted by a power law in the power density spectra (the exponents of the power were different for the two observations). LFN (above 0.5 Hz) was exclusively observed during the 1985 observations; its strength increased from $\lesssim 1.5$ to 3 per cent as the spectral state changed from the normal branch to the horizontal branch. This behaviour is very similar to that in Cyg X-2 and GX 5−1 which also show approximately 5–6 Hz QPO in the normal branch, LFN above 0.5 Hz in the horizontal branch with associated high-frequency (20–50 Hz) intensity-dependent QPO, and VLFN in both branches.

It thus appears that GX 340+0 is similar in its bimodal QPO/spectral-state behaviour to Cyg X-2 and GX 5−1 (and possibly to GX 17+2; Hasinger 1987b), and we suspect that high-frequency QPO was present during the 1985 observations when the source was in the horizontal branch state, but that we were unable to detect it because of the 31 ms time resolution. Future observations will be able to confirm our expectations.

In order to compare the QPO, LFN and VLFN characteristics, and their relation to the spectral states, it would greatly help if future analyses, where possible, be done in a unified way, comparing spectral and timing properties in relation to specific portions of the spectral branches. This would also facilitate theoretical work; the origin of QPO is still unknown.

Acknowledgments

WHGL acknowledges support of the United States National Aeronautics and Space Administration (contract NAS8-571). He and JvP thank the directors of the Max-Planck-Institut für Extraterrestrische Physik for their hospitality.

References

Branduardi, G., Kylafis, N. D., Lamb, D. Q. & Mason, K. O., 1980. *Astrophys. J.,* **235,** L153.
Cooke, B., Stella, L. & Ponman, T., 1985. *IAU Circ. No. 4116.*
Ercan, E. N. & Cruise, A. M., 1984. *Mon. Not. R. astr. Soc.,* **209,** 271.
Forman, W., Jones, C., Cominsky, L., Julien, P., Murray, S., Peters, G., Tananbaum, H. & Giacconi, R., 1978. *Astrophys. J. Suppl.,* **38,** 357.
Gorenstein, P., 1975. *Astrophys. J.,* **198,** 95.
Grindlay, J. E. & Seaquist, E. R., 1986. *Astrophys. J.,* **310,** 172.
Hasinger, G., 1987a. In: *The Origin and Evolution of Neutron Stars, IAU Symp. No. 125,* p. 333, eds Helfand, D. J. & Huang, J. H., Reidel, Dordrecht, Holland.
Hasinger, G., 1987b. *Astr. Astrophys.,* in press.
Hasinger, G., Langmeier, A., Sztajno, M., Truemper, J., Lewin, W. H. G. & White, N. E., 1986. *Nature,* **319,** 469.
Hertz, P. & Grindlay, J. E., 1984. *Astrophys. J.,* **282,** 118.
Jones, C., 1977. *Astrophys. J.,* **214,** 856.
Leahy, D. A., Darbro, W., Elsner, R. F., Weisskopf, M. C., Sutherland, P. G., Kahn, S. & Grindlay, J. E., 1983. *Astrophys. J.,* **266,** 160.
Lewin, W. H. G., 1987a. In: *The Physics of Accretion onto Compact Stars, Lecture Notes in Physics,* Vol. 266, p. 177, eds Mason, K. O., Watson, M. G. & White, N. E., Springer-Verlag, Berlin.

Lewin, W. H. G., 1987b. In: *The Origin and Evolution of Neutron Stars, IAU Symp. No. 125,* p. 363, eds Helfand, D. J. & Huang, J. H., Reidel, Dordrecht, Holland.

Lewin, W. H. G. & van Paradijs, J., 1986. *Comm. Astrophys.,* **11,** 127.

Lewin, W. H. G., van Paradijs, J., Jansen, F., van der Klis, M., Sztajno, M. & Truemper, J., 1985. *IAU Circ. No. 4101.*

Lewin, W. H. G., van Paradijs, J., Hasinger, G., Penninx, W. H., Langmeier, A., van der Klis, M., Jansen, F., Basinska, E. M., Sztajno, M. & Truemper, J., 1987a. *Mon. Not. R. astr. Soc.,* **226,** 383.

Lewin, W. H. G., van Paradijs, J., van der Klis, M., Jansen, F., Basinska, E. M., Langmeier, A., Sztajno, M. & Truemper, J., 1987b. *Mon. Not. R. astr. Soc.,* submitted.

Makishima, K., 1986. *ISAS Research Note No. 313.*

Margon, B., Bowyer, S., Lampton, M. & Cruddace, R., 1971. *Astrophys. J.,* **169,** L45.

Markert, T. H., Winkler, P. F., Laird, F. N., Clark, G. W., Hearn, D. R., Sprott, G. F., Li, F. K., Bradt, H. V., Lewin, W. H. G. & Schnopper, H. W., 1979. *Astrophys. J. Suppl.,* **39,** 573.

Norris, J. P. & Wood, K. S., 1987. *Astrophys. J.,* **312,** 732.

Parsignault, D. R. & Grindlay, J. E., 1978. *Astrophys. J.,* **225,** 970.

Penninx, W., Hasinger, G., Lewin, W. H. G., van Paradijs, J., Jansen, F., Langmeier, A., Sztajno, M., Truemper, J. & van der Klis, M., 1987. *Mon. Not. R. astr. Soc.,* to be submitted.

Ponman, T., 1982. *Mon. Not. R. astr. Soc.,* **201,** 769.

Priedhorsky, W., Hasinger, G., Lewin, W. H. G., Middleditch, J., Parmar, A., Stella, L. & White, N. E., 1986. *Astrophys. J.,* **306,** L91.

Rappaport, S., Zaumen, W., Doxsey, R. & Mayer, W., 1971. *Astrophys. J.,* **169,** L93.

Ryter, C., Cesarsky, C. J. & Audouze, J., 1975. *Astrophys. J.,* **198,** 103.

Shibazaki, N. & Mitsuda, K., 1984. In: *High Energy Transients in Astrophysics,* p. 49, ed. Woosley, S. E., American Institute of Physics.

Stella, L., 1986. In: *Plasma Penetration into Magnetospheres,* p. 199, eds Kylafis, N., Papamastorakis, J. & Ventura, J., Crete University Press.

Stella, L., Parmar, A. N. & White, N. E., 1987. *Astrophys. J.,* submitted.

Tennant, A., 1987. *Mon. Not. R. astr. Soc.,* **226,** 963.

Turner, M. J. L., Smith, A. & Zimmermann, H. U., 1981. *Space Sci. Rev.,* **30,** 513.

van der Klis, M., 1987. In: *The Physics of Accretion onto Compact Stars, Lecture Notes in Physics,* Vol. 266, p. 157, eds Mason, K. O., Watson, M. G. & White, N. E., Springer-Verlag, Berlin.

van der Klis, M., Jansen, F., van Paradijs, J., Lewin, W. H. G., Truemper, J., van den Heuvel, E. P. J. & Sztajno, M., 1985. *Nature,* **316,** 225.

van der Klis, M., Jansen, F., van Paradijs, J., Lewin, W. H. G., Sztajno, M. & Truemper, J., 1987a. *Astrophys. J.,* **313,** L19.

van der Klis, M., Stella, L., White, N. E., Jansen, F. & Parmar, A. N., 1987b. *Astrophys. J.,* **316,** 411.

van Paradijs, J., Lewin, W. H. G., Hasinger, G., van der Klis, M., Penninx, W., Sztajno, M., Langmeier, A. & Jansen, F., 1987. *IAU Circ. No. 4308.*

Warwick, R. S., Marshall, N., Fraser, G. W., Watson, M. G., Lawrence, A., Page, C. G., Pounds, K. A., Ricketts, M. J., Sims, M. R. & Smith, A., 1981. *Mon. Not. R. astr. Soc.,* **197,** 865.

Wood, K. S., Meekins, J. F., Yentis, D. J., Smathers, H. W., McNutt, D. P., Bleach, R. D., Byram, E. T., Chubb, T. A. & Friedman, H., 1984. *Astrophys. J. Suppl.,* **56,** 507.